HOSTED BY

Available online at www.sciencedirect.com

ScienceDirect

Journal of Otology 10 (2015) 13–17

www.journals.elsevier.com/journal-of-otology/

Optimizing CT for the evaluation of vestibular aqueduct enlargement: Inter-rater reproducibility and predictive value of reformatted CT measurements

Misun Hwang [a], Ryan Marovich [b], Samuel S. Shin [c], David Chi [d], Barton F. Branstetter IV [a,b,*]

[a] Department of Radiology, University of Pittsburgh Medical Center, USA
[b] Department of Otolaryngology, University of Pittsburgh Medical Center, USA
[c] Department of Neurosurgery, University of Pittsburgh Medical Center, USA
[d] Department of Otolaryngology, Children's Hospital of Pittsburgh, USA

Received 18 May 2015; accepted 14 July 2015

Abstract

Enlarged vestibular aqueduct (EVA), the most frequent identifiable cause of congenital hearing loss, is evaluated with high-definition multi-detector CT in the axial plane. Our purpose was to determine which reformatted CT measurements are most reproducible. Seven multiplanar reformatted images were created for each of the 64 temporal bones in patients with EVA. Intraclass correlation coefficients (ICC) were used to assess inter-observer variability, and both linear regression and ROC analyses were used to compare the measurements with severity of hearing loss, as assessed by pure tone audiometry. All seven measurements had excellent inter-observer variability, with average-measure ICC ranging from 0.92 to 0.98. There was no statistically significant correlation between the radiologic degree of aqueduct enlargement and severity of hearing loss using any of the seven measurements; ROC analyses revealed areas under the curves ranging from 0.57 to 0.73. Optimal accuracy was obtained with a threshold of 1.75 mm as measured at the aqueductal aperture in the Pöschl plane, with sensitivity of 0.75 and specificity of 0.63. Although the radiologic measurement may not serve as a reliable tool for assessing severity of EVA, Pöschl plane reformatting has proven to be better than conventional axial acquisition plane for identifying patients with clinically significant hearing loss.

Keywords: Enlarged vestibular aqueduct; Hearing loss; Computed tomography; Reformat

1. Introduction

Enlarged vestibular aqueduct (EVA) is the most common pathologic imaging finding in children undergoing CT evaluation for sensorineural hearing loss (Urman and Talbot, 1990; Mafee et al., 1992). Developing an imaging technique which permits accurate measurement of the vestibular aqueduct in consideration of its 3D morphology therefore has important clinical indications.

After the discovery of enlarged vestibular aqueduct (EVA) during a temporal bone dissection by Mondini (1791). A large-scale study examining 3700 patients with EVA followed in 1978 which defined EVA as greater than 1.5 mm at the midpoint and 2 mm at the external aperture of the vestibular aqueduct on the axial plane (Valvassori and Clemis, 1978). The established criterion has since been used to diagnose EVA on CT. A more recent study by Boston et al., however, defined

* Corresponding author. 3950 Presby South Tower, 200 Lothrop Street, Pittsburgh, PA 15213, USA. Tel.: +1 412 647 3530; fax: +1 412 647 5359.
E-mail address: branbf@upmc.edu (B.F. Branstetter).
Peer review under responsibility of PLA General Hospital Department of Otolaryngology Head and Neck Surgery.

http://dx.doi.org/10.1016/j.joto.2015.07.004

EVA as greater than 1.9 mm at the external aperture and/or greater than 0.9 mm at the midpoint in an axial CT scan of 107 children (Boston et al., 2007). Given the inconsistent results, continued efforts to solidify the imaging criterion for diagnosing EVA is needed.

The vestibular aqueduct has an inverted J shape with a short descending proximal segment and a longer descending distal segment (Valvassori and Clemis, 1978; Becker et al., 1983; Pimontel-Appel and Ettore, 1980; Wilbrand et al., 1974; Kodama and Sando, 1982; Dimopoulos et al., 1996; Kraus and Dubois, 1979). The proximal segment arising from the medial wall of the vestibule curves superiorly and medially up to a bend, the isthmus, while the distal straight segment ends as the external aperture on the posterior surface of the petrous pyramid and is shaped like a compressed cone (Valvassori and Clemis, 1978). This complex anatomy makes measurement of the shortest diameter of the aqueduct difficult in the axial plane that is routinely used for the evaluation of EVA.

Multidetector spiral CT scanner permits reformat of the vestibular aqueduct in any desired plane (Venema et al., 1999). With this advantage, Curtin et al. utilized the Pöschl projection, defined as approximately 45° from either the sagittal or coronal planes or perpendicular to the axis of the pyramid, and demonstrated improved imaging accuracy over the axial plane. The study measured EVA with improved accuracy using the Pöschl projection than the axial plane. Another study utilized the coronal image and showed improved reproducibility as compared to the axial plane and slightly larger than the previously reported anatomic measurements of EVA (Murray et al., 2000).

The purpose of this study was to elucidate the optimal imaging plane with the highest diagnostic accuracy for prediction of severity of sensorineural hearing loss in patients with EVA, and to determine whether CT-derived measurements were reproducible among different readers.

2. Materials and methods

2.1. Subjects

A total of 179 temporal bone CTs with sensorineural hearing loss as the indication, acquired from 2001 to 2013, were retrospectively collected after approval by the University of Pittsburgh Institutional Review Board. Of the 179 temporal bone CTs, only 55 cases (31%) with available hearing test results as well as no other anatomic abnormalities on CT were analyzed. Excluded cases had no available pure tone audiometry results (n = 83), no available temporal bone CT (n = 12), no accessible study (n = 5), preexisting cochlear and/or vestibular anomaly (n = 5), myringosclerosis (n = 1), labyrinthitis (n = 1), motion degradation (n = 4), patients less than 1 year of age (n = 5), and normal caliber vestibular aqueduct (n = 4). Patients under the age of 3 were also excluded since vestibular aqueduct continues to grow after birth but reaches the adult size by the age of 3 (Fujita and Sando, 1994).

2.2. Data acquisition

CT of the temporal bones were acquired using a 64-channel CT scanner (Siemens, Erlangen, Germany) with 0.5-mm collimation, 0.5-mm thickness, 320 mAs, and 120 kVp. Bone reconstruction kernel with window/level setting of 4000/800, 0.5-mm section thickness, 0.5-mm increments, and a FOV of 100, with a matrix size of 512 × 512 were used. The axial data were transferred to VitreaCore (Vital Images, Inc.), a commercially-available 3D reformatting software, for postprocessing.

2.3. Image evaluation

Three observers of varying levels of training created reformatted images and made independent measurements of

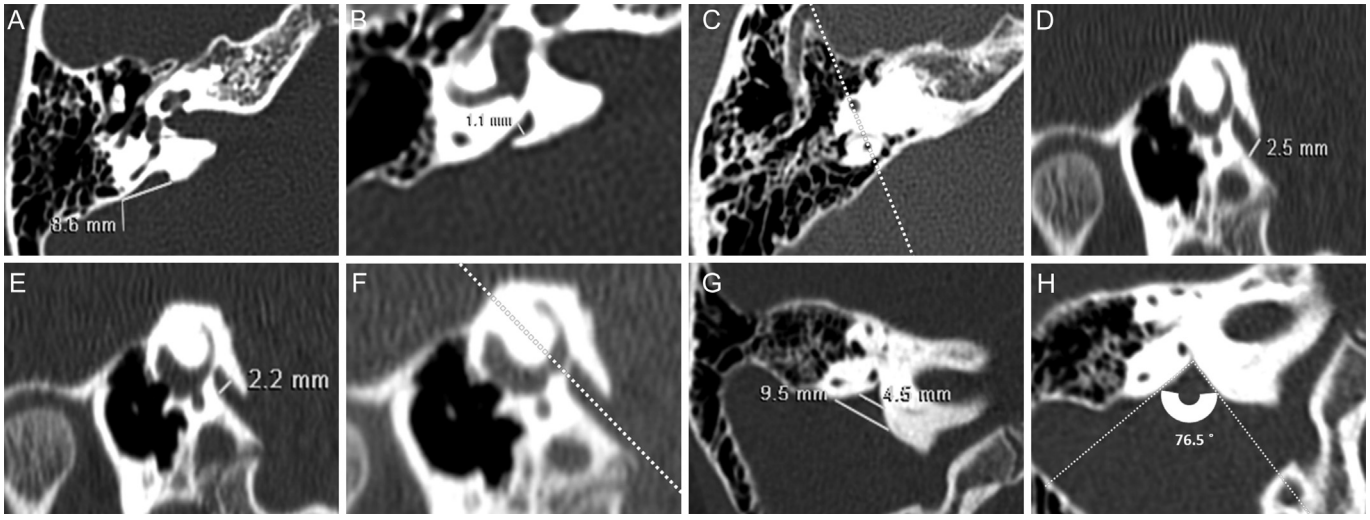

Fig. 1. Receiver operating characteristic (ROC) curve. Sensitivity and specificity values of the vestibular aqueduct diameter measured on seven CT reconstruction planes: AxialE (axial plane external aperture), axialI (axial plane midpoint), PöschlE (Pöschl plane external aperture), PöschlI (Pöschl plane midpoint), AOE (axial oblique external aperture), AOI (axial oblique midpoint), angle (angle on axial oblique plane).

the vestibular aqueduct. One observer was a CAQ-certified neuroradiologist with 10 years of dedicated experience in head and neck imaging (BB); one observer was a PGY4 radiology resident (MH), and one observer was PGY2 neurosurgery resident (SS). The planes of reformat were the acquisition axial plane, the plane of Pöschl (parallel to the loop of the superior semicircular canal), and the axial oblique plane (along the axis of the vestibular aqueduct as seen in the plane of Pöschl). Seven measurements of the enlarged vestibular aqueducts were obtained in these three planes: conventional axial plane (external aperture and midpoint), Pöschl plane (external aperture and midpoint) (Curtin et al., 2003), axial oblique plane (external aperture and midpoint), and aqueductal angle (angle formed by the lateral walls of the aqueduct on the axial oblique plane). These measurements and planes of reformat are demonstrated in Fig. 1. The midpoint of the postisthmic segment was defined as halfway between the external aperture and the common crus by Valvassori and Dobben (1984). Since the simultaneous visualization of the external aperture and the common crus on the axial plane is not feasible, the midpoint was approximated by scrolling between the common crus and the external aperture. Pure tone audiometry (PTA) data of one or both ears of each patient were obtained by review of the electronic medical record.

2.4. Statistical analysis

For assessment of inter-observer variability, intra-class coefficients (ICC) were calculated. Pearson's *r* was used to evaluate correlation between the seven radiologic measurements and the air-bone gap on PTA. A receiver operator characteristic (ROC) curve was generated for each measurement, by using an air-bone gap greater than 25 dB as the threshold for clinically-relevant hearing loss. For the ROC curves, the average measurement of the three observers was utilized.

3. Results

Comparison of the seven reformatted measurements revealed excellent inter-observer variability, with average-measure ICC ranging from 0.92 to 0.98 (Table 1). There were no statistically significant correlations between the radiologic degree of aqueduct enlargement and the severity of hearing loss using any of the seven measurements. ROC analyses revealed areas under the curves ranging from 0.57 to 0.73 (Fig. 2, Table 1). Optimal predictive accuracy was obtained with a threshold of 1.75 mm as measured at the aperture in the Pöschl plane, which resulted in a sensitivity of 0.75 and a specificity of 0.63 for the prediction of hearing loss >25 dB.

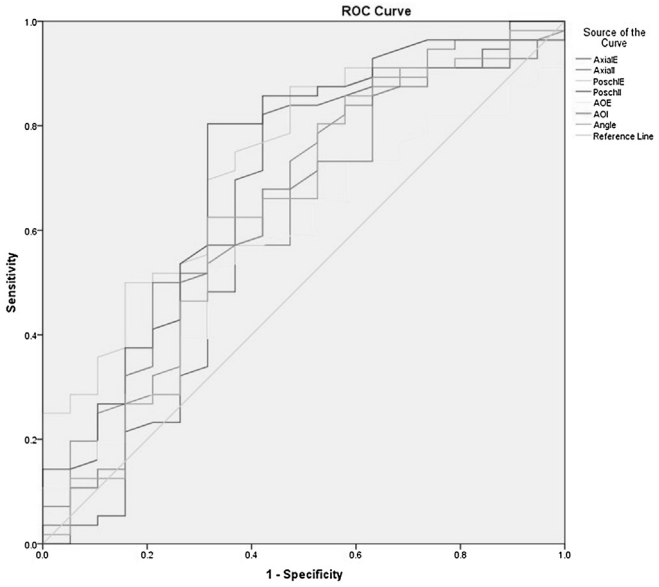

Fig. 2. Instructions for obtaining Reformatted CT Measurements of the Vestibular Aqueduct. A. Begin with the axial slice through the vestibular aqueduct. Obtain standard axial measurements of the external aperture. B. Measure the midpoint on the axial slice after scrolling to determine the approximate location. C. On a more superior axial slice, prescribe a sagittal oblique plane through the anterior and posterior limbs of the superior semicircular canal (this is the plane of Pöschl). D. In the plane of Pöschl, measure the external aperture. E. Measure the midpoint on the plane of Pöschl after scrolling to determine the approximate location. F. While in the plane of Pöschl, prescribe an axial oblique plane along the course of the enlarged aqueduct. G. Measure the external aperture and midpoint in the axial oblique plane. H. Measure the angle formed by the lateral walls of the aqueduct on the axial oblique plane.

4. Discussion

Evaluation of the seven reformatted measurements of EVA in this study revealed maximum accuracy with the Pöschl plane albeit with suboptimal specificity and sensitivity. Although the radiologic measurement may not serve as a reliable tool for assessing severity of EVA, Pöschl reformatting has proven to be better than conventional axial acquisition plane.

Given the J-shaped appearance of the aqueduct in 3D dimensions, it is challenging to standardize the reformatted

Table 1
Reproducibility and Accuracy of reformatted CT measurements. ICC = Intra-class coefficient. ROC = Receiver Operator Charactersitic Curve. Axial E = axial plane external aperture, Axial I = axial plane midpoint, Pöschl E = Pöschl plane external aperture, Pöschl I = Pöschl plane midpoint, AOE = axial oblique external aperture, AOI = axial oblique midpoint, Angle = angle on axial oblique plane.

	Axial E	Axial I	Pöschl E	Pöschl I	AOE	AOI	Angle
Single-measures ICC	0.93	0.86	0.92	0.90	0.87	0.79	0.82
Average-measures ICC	0.98	0.95	0.97	0.97	0.95	0.92	0.93
Area under ROC curve	0.63	0.65	0.73	0.72	0.57	0.63	0.63

plane which offers maximum accuracy. We therefore evaluated seven different reformatted measurements to assess for which offers the maximum accuracy. With further adaptation of the Pöschl plane, the present study generated for the first time an axial oblique plane along the course of the aqueduct. Both the external aperture and midpoint measurements were made on this plane in addition to the angle measurement between the lateral walls of the aqueduct. As compared to Pöschl reformatting, however, measurements in the axial oblique plane resulted in lower accuracy, largely due the variability in appearance of the axial oblique reformat. Comparison of the standard axial, Pöschl, and axial oblique measurements revealed a maximum accuracy when measuring the external aperture in Pöschl plane (sensitivity of 0.75 and specificity of 0.63).

Our findings are in concert with the prior study by Curtin et al. which demonstrated a superior delineation of EVA with the 45 oblique or Pöschl planes as compared to the conventional axial plane (Curtin et al., 2003). Further studies other than Curtin et al. have followed to establish an optimal diagnostic criterion for EVA, including a study using the coronal plane to show improved consistency in aqueduct measurement than on axial plane and slightly larger than the previously reported anatomic measurements of EVA (Murray et al., 2000). Despite the efforts, however, deriving a single plane on which to depict the 3D morphology of EVA has undoubtedly been difficult.

In this study, we also found a lack of correlation between the radiologic degree of aqueduct enlargement and severity of hearing loss using any of the seven measurements. Few prior studies also failed to demonstrate any correlation between hearing loss and sac or duct size (Berrettini et al., 2005; Grimmer and Hedlund, 2007). On the other hand, Antonelli et al. found that the amount of enlargement and morphology of the aqueduct correlated highly with the severity of hearing loss (Antonelli et al., 1998). Lai et al. similarly showed that the midpoint and opercular diameters of the enlarged vestibular aqueduct correlated with the frequency and severity of hearing loss fluctuations (Lai and Shiao, 2004). In regard to the contradictory findings, further studies on this topic with larger cohort and less selection bias may provide a conclusive answer.

There are several limitations in the study. Relatively a small number of patients with available audiograms were evaluated, decreasing the power of study. Exclusion of those without audiogram results could have decreased the number of true negatives and biased the study sample toward cases of clinically obvious hearing loss. In addition, the study evaluated only seven of the infinite number of reformatted measurements. An inverted J shape to the vestibular aqueduct cannot be entirely depicted on a single reformatted plane. Either a triangle to bell-shaped appearance of the vestibular aqueduct, as appreciated on the axial oblique plane, further complicates the measurement (Fig. 3). In such case, measurement of the area or circumference of the aqueduct on the measurement pane could prove to be a more reliable method.

In summary, our results demonstrate the superiority of Pöschl plane over the conventional axial plane in measuring EVA with maximum accuracy. Improving the current diagnostic algorithm for EVA on CT is clinically important given the routine acquisition of temporal bone CTs at initial presentation of sensorineural hearing loss.

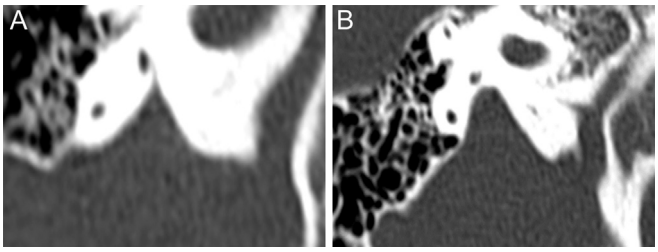

Fig. 3. Variability of the Aqueduct Shape in the Axial Oblique Plane. A shows a cone-shaped vestibular aqueduct while B shows a bell-shaped vestibular aqueduct.

5. Conclusion

This study has shown that Pöschl reformatting permits measurement of EVA with higher predictive accuracy for hearing loss than the conventional axial plane. Also, these CT measurements have excellent inter-observer reliability, so highly experienced users are not necessary for accurate measurement.

Conflicts of interest

There are no conflicts of interest in the manuscript.

Sources of funding

No outside funding support was provided for this study.

References

Antonelli, P.J., Nall, A.V., Lemmerling, M.M., Mancuso, A.A., Kubilis, P.S., 1998. Hearing loss with cochlear modiolar defects and large vestibular aqueducts. Am. J. Otol. 19, 306–312.

Becker, T.S., Vignaud, J., Sultan, A., et al., 1983. The vestibular aqueduct in congenital deafness: evaluation by the axial projection. Radiology 149, 741–744.

Berrettini, S., Forli, F., Bogazzi, F., Neri, E., Salvatori, L., Casani, A.P., et al., 2005. Large vestibular aqueduct syndrome: audiological, radiological, clinical, and genetic features. Am. J. Otolaryngol. 26, 363–371.

Boston, M., Halsted, M., Meinzen-Derr, J., et al., 2007. The large vestibular aqueduct: a new definition based on audiologic and computed tomography correlation. Otolaryngol. Head Neck Surg. 136, 972–977.

Curtin, H.D., Sanelli, P.C., Som, P.M., 2003. Temporal Bone: Embryology and Anatomy, fourth ed. Mosby, St. Louis.

Dimopoulos, P.A., Smedby, O., Wilbrand, H.F., 1996. Anatomical variations of the human vestibular aqueduct. Part I. A radioanatomical study. Acta Radiol. Suppl. 403, 21–32.

Fujita, S., Sando, I., 1994. Postnatal development of the vestibular aqueduct in relation to the internal auditory canal. Computer-aided three-dimensional reconstruction and measurement study. Ann. Otol. Rhinol. Laryngol. 103, 719–722.

Grimmer, J.F., Hedlund, G., 2007. Vestibular symptoms in children with enlarged vestibular aqueduct anomaly. Int. J. Pediatr. Otorhinolaryngol. 71, 275–282.

Kodama, A., Sando, I., 1982. Dimensional anatomy of the vestibular aqueduct and the endolymphatic sac (rugose portion) in human temporal bones. Statistical analysis of 79 bones. Ann. Otol. Rhinol. Laryngol. Suppl. 96, 13−20.

Kraus, E.M., Dubois, P.J., 1979. Tomography of the vestibular aqueduct in ear disease. Arch. Otolaryngol. 105, 91−98.

Lai, C.C., Shiao, A.S., 2004. Chronological changes of hearing in pediatric patients with large vestibular aqueduct syndrome. Laryngoscope 114, 832−838.

Mafee, M.F., Charletta, D., Kumar, A., et al., 1992. Large vestibular aqueduct and congenital sensorineural hearing loss. AJNR Am. J. Neuroradiol. 13, 805−819.

Mondini, C., 1791. Anatomica surdi nati sectio, vol. 7. De Bononiensi Scientarium et Artium Instituto atque Academia Commenarii, Banoniae, p. 419.

Murray, L.N., Tanaka, G.J., Cameron, D.S., Gianoli, G.J., 2000. Coronal computed tomography of the normal vestibular aqueduct in children and young adults. Arch. Otolaryngol. Head Neck Surg. 126, 1351−1357.

Pimontel-Appel, B., Ettore, G.C., 1980. Poschl positioning and the radiology of Meniere's disease. J. Belge Radiol. 63, 359−367.

Urman, S.M., Talbot, J.M., 1990. Otic capsule dysplasia: clinical and CT findings. Radiogr. Rev. Publ. Radiol. Soc. N. Am. Inc. 10, 823−838.

Valvassori, G.E., Clemis, J.D., 1978. The large vestibular aqueduct syndrome. Laryngoscope 88, 723−728.

Valvassori, G.E., Dobben, G.D., 1984. Multidirectional and computerized tomography of the vestibular aqueduct in Meniere's disease. Ann. Otol. Rhinol. Laryngol. 93, 547−550.

Venema, H.W., Phoa, S.S., Mirck, P.G., et al., 1999. Petrosal bone: coronal reconstructions from axial spiral CT data obtained with 0.5-mm collimation can replace direct coronal sequential CT scans. Radiology 213, 375−382.

Wilbrand, H.F., Rask-Andersen, H., Gilstring, D., 1974. The vestibular aqueduct and the para-vestibular canal. An anatomic and roentgenologic investigation. Acta Radiol. Diagn. 15, 337−355.